7-2012

Magnetic and magnetoelastic properties of Zn-doped cobalt-ferrites —$CoFe_{2-x}Zn_xO_4$ (x = 0, 0.1, 0.2, and 0.3)

Nalla Somaiah
University of Hyderabad

Tanjore V. Jayaraman
University of Nebraska-Lincoln, tjayaraman2@unl.edu

P. A. Joy
National Chemical Laboratory, Pune, India

Dibakar Das
National Chemical Laboratory, Pune, India, dibakar1871@gmail.com

Published in *Journal of Magnetism and Magnetic Materials* 324:14 (July 2012), pp. 2286–2291; doi: 10.1016/j.jmmm.2012.02.116

Submitted December 16, 2011; revised February 11, 2012; published online March 6, 2012.

Magnetic and magnetoelastic properties of Zn-doped cobalt-ferrites—$CoFe_{2-x}Zn_xO_4$ (x = 0, 0.1, 0.2, and 0.3)

Nalla Somaiah,[1] Tanjore V. Jayaraman,[2] P.A. Joy,[3] and Dibakar Das[1]

1. School of Engineering Sciences and Technology, University of Hyderabad, Hyderabad 500046, India
2. Department of Mechanical and Materials Engineering, University of Nebraska–Lincoln, Lincoln, NE 68588, USA
3. Materials Chemistry Division, National Chemical Laboratory, Pune 411008, India

Corresponding author — D. Das, tel 91 40 23134454, email ddse@uohyd.ernet.in ; dibakar1871@gmail.com

Abstract

Cobalt-ferrite ($CoFe_2O_4$) based materials are suitable candidates for magnetomechanical sensor applications owing to a strong sensitivity of their magnetostriction to an applied magnetic field. Zn-doped cobalt-ferrites, with nominal compositions $CoFe_{2-x}Zn_xO_4$ (x = 0–0.3), were synthesized by auto-combustion technique using Co- , Fe- , and Zn-nitrate as precursors. X-ray spectra analysis and Transmission electron microscopy studies revealed that the as-prepared powders were comprised of nano-crystalline (~25–30 nm) cubic-spinel phase with irregularly-shaped grains morphology along with minor impurity phases. Calcination (800 °C for 3 h) of the precursor followed by sintering (1300 °C for 12 h) resulted in a single phase cubic-spinel structure with average grain size ~2–4 μm, as revealed from scanning electron micrographs. The magnitude of coercive field decreases from ~540 Oe for x = 0 to 105 Oe for x = 0.30. Saturation magnetization initially increases and peaks to ~87 emu/g for x = 0.2 and then decreases. The peak value of magnetostriction monotonically decreases with increasing Zn content in the range 0.0–0.3; however the piezomagnetic coefficient ($d\lambda/dH$) reaches a maximum value of 105×10^{-9} Oe^{-1} for x = 0.1. The observed variation in piezomagnetic coefficient in the Zn substituted cobalt ferrite is related to the reduced anisotropy of the system. The Zn-doped cobalt-ferrite (x = 0.1) having high strain derivative could be a potential material for stress sensor application.

Keywords: Cobalt-ferrite, Magnetic-properties, Magnetostriction

1. Introduction and background

Ferrimagnetic cubic spinels, known as ferrites, possess magnetic and electrical properties that are of significant importance in many technological applications at room temperature such as data storage devices, magnetic sensors, actuators, targeted drug delivery, medical diagnosis, etc. [1–4]. Co-ferrites ($CoFe_2O_4$) are extensively studied because of their interesting properties such as cubic magnetocrystalline anisotropy, high coercivity, moderate saturation-magnetization, high chemical stability, wear resistance, and electrical insulation [5–8]. Their application in various field arise from their ability to distribute the cations among available sublattices, tetrahedral, and octahedral sites [9]. For non-contact stress sensor applications Co-ferrite is identified as a suitable material. Co-ferrites have large strain derivative (higher than Terfenol-D), better corrosion resistance, no eddy current loss, and low cost (rare-earth free) [4]. Some of their properties can be manipulated not only by choosing a suitable dopant (to form a ternary cations spinel) but also by choosing a suitable synthesis method. Among the various synthesis methods, especially the wet chemical methods, the auto-combustion method has numerous advantages including inexpensive precursors, low external energy consumption, and simple equipment requirement. The resulting powders are nanosized, homogeneous, and are of high purity [10]. A lot of work has been reported in the literature about different types of doped Co-ferrites synthesized by various methods [11–21]. In this work we investigate the magnetic and magnetoelastic properties of Zn substituted (for Fe) cobalt ferrite, $CoFe_{2-x}Zn_xO_4$ (x = 0, 0.1, 0.2, and 0.3), synthesized by the auto-combustion method.

2. Materials and methods

Zn doped cobalt-ferrites with nominal compositions $CoFe_{2-x}Zn_xO_4$ (x = 0, 0.1, 0.2, and 0.3) were synthesized by a novel auto-combustion technique [22, 23]. The precursors used in the synthesis were $Co(NO_3)_2.6H_2O$, $Fe(NO_3).9H_2O$, and $Zn(NO_3)_2.6H_2O$; glycine was added as the fuel. The as-prepared powders were calcined at 800 °C for 3 h in order to obtain the desired single phase of cubic-spinel and eliminate any unreacted precursors. The calcined powder was pressed into pellets of dimension ~10 mm × ~9 mm (length × diameter) using a uniaxial hydraulic press at an applied pressure of

200 MPa. The sintering of the green pellets was performed at 1300 °C for 12 h. The as-prepared, calcined, and sintered ferrites were analyzed by a Bruker D8 Advance X-ray Diffractometer with θ–2θ geometry using Cu K_α radiation. While Transmission Electron Microscopy (TEM) was performed on as-prepared and calcined powders using FEI Tecnai T20G^2 S TWIN TEM; the Scanning Electron Microscopy (SEM) was performed on sintered ferrites using Carl Zeiss Ultra 55 FE-SEM. The magnetic characterization was performed on the sintered pellets using a Lakeshore (Model 7407) Vibrating Sample Magnetometer (VSM) in fields up to 2 T at ambient temperature (~298 K). The accuracy of the magnetization measurement was within ±1%. The magnetostriction measurement of the sintered pellets was performed by strain gage technique [24]; the measurement was performed on the flat surfaces of samples using a strain gage (Vishay Micro-Measurement—EK-09-062AP-350-SE) with a strain indicator, and the magnetic field was applied using an electromagnet.

3. Results and discussion

The x-ray diffraction spectra (Figure 1a) of the as-prepared Zn doped cobalt-ferrites, $CoZn_xFe_{2-x}O_4$ (x = 0, 0.1, 0.2, and 0.3), shows the presence of desired phase of cubic-spinel along with some minor amount of impurity phase(s). The broader peaks of the spinel phase suggest the presence of cubic-spinel phase in nanocrystalline form. The crystallite size was determined from the full-width at half-maxima (FWHM) of the strongest reflection (Voigt function fit) [25], the (311) peak, using the Scherrer's formula [26]; $t = 0.9\lambda/(w-w_i)\cos\theta_B$, where t is the average diameter in nm, w is the half-intensity width of the relevant diffraction peaks, w_i represents the half-intensity width due to instrumental broadening, λ is the wavelength of x-ray radiation, and θ_B is the Bragg's diffraction angle. The crystallite size were ~46 nm (±10 nm), ~52 nm, ~41 nm, and ~43 nm for as-prepared $CoFe_2O_4$, $CoFe_{1.9}Zn_{0.1}O_4$, $CoFe_{1.8}Zn_{0.2}O_4$, and $CoFe_{1.7}Zn_{0.3}O_4$ respectively. The TEM micrographs (Figure 1b & c) of as-prepared $CoFe_2O_4$ shown as a representative, suggests the presence of irregularly shaped grains of crystalline cubic-spinel phase with grain size ~25–30 nm. The observed differences in the crystallite size between the XRD spectra and the TEM micrograph is likely due to the limited sampling region allowed by TEM. However both x-ray spectra and the TEM measurements suggest that auto-combustion technique is a suitable method for synthesizing nanostructured Zn doped cobalt-ferrites, $CoZn_xFe_{2-x}O_4$ (x = 0, 0.1, 0.2, and 0.3).

Figure 2 shows the x-ray diffraction spectra and TEM micrographs of the calcined (calcination of as-prepared powders) Zn doped ferrites, $CoZn_xFe_{2-x}O_4$ (x = 0, 0.1, 0.2, and 0.3). The absence of any impure phase(s) in the calcined powder, as seen in the x-ray spectra (Figure 2a), suggests the completion of the cubic-spinel phase formation during the calcinations process. The peaks of the spinel phase after calcination are less broad as compared to their as-prepared counterparts. The crystallite size, determined by Scherrer's formula, were ~88 nm (±10 nm), ~87 nm, ~81 nm, and ~82 nm for calcined $CoFe_2O_4$, $CoFe_{1.9}Zn_{0.1}O_4$, $CoFe_{1.8}Zn_{0.2}O_4$, and $CoFe_{1.7}Zn_{0.3}O_4$ respectively. The observed increase in crystallite size is likely due to the particle growth as a result of solid state diffusion during the calcinations process, as expected. The TEM micrograph (Figure 2b) of calcined $CoFe_2O_4$ shown as a representative, suggests the presence of highly regular in shape grains with grain size ~100 nm. The agglomeration seen in the picture is probably due to improper sonication during TEM sample preparation. The grain size observed from the TEM image matches closely with the crystallite sizes calculated by Scherrer's formula.

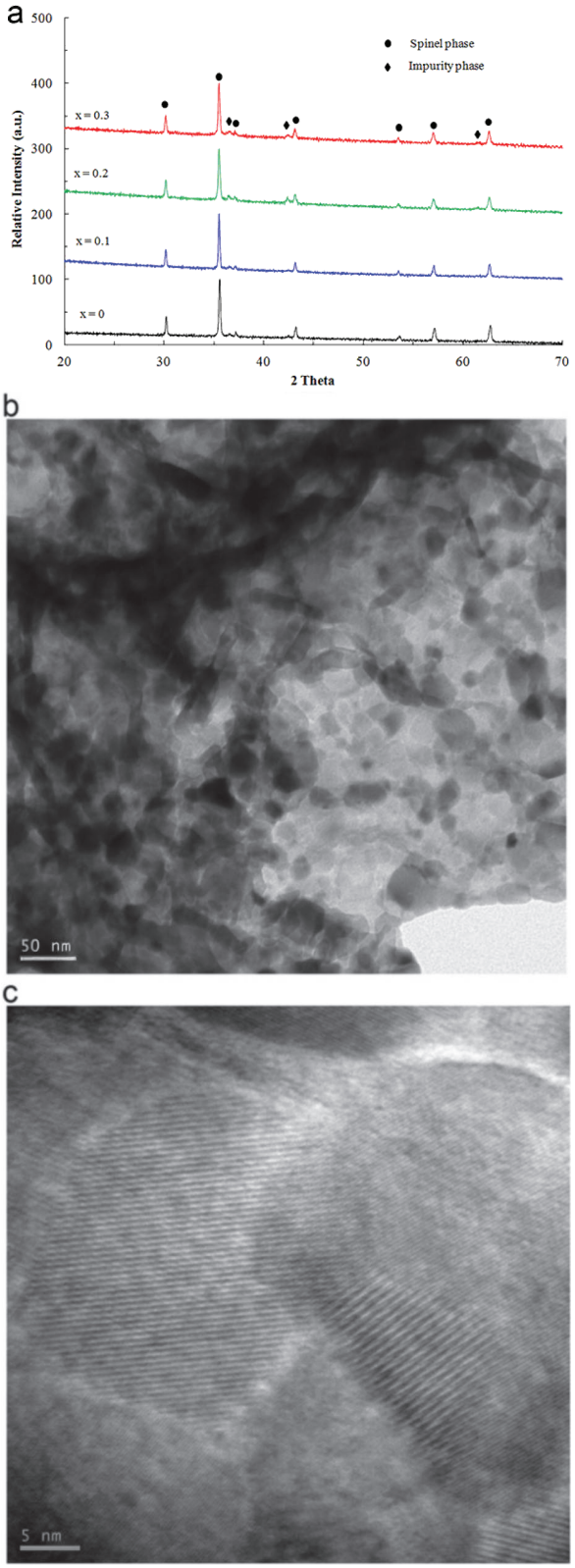

Figure 1. (a) X-ray diffraction spectra of as-prepared $CoZn_xFe_{2-x}O_4$, (x = 0, 0.1, 0.2, and 0.3) prepared by the auto-combustion method; (b) Bright-field and (c) High-resolution TEM image of as-prepared $CoFe_2O_4$.

Figure 3 shows the x-ray diffraction spectra for the sintered (1300 °C for 12 h) Zn doped Co-ferrites, $CoZn_xFe_{2-x}O_4$ (x = 0, 0.1, 0.2, and 0.3). The spectra reveal a cubic spinel structure (space group $Fd3m$) without any ambiguous reflections. The

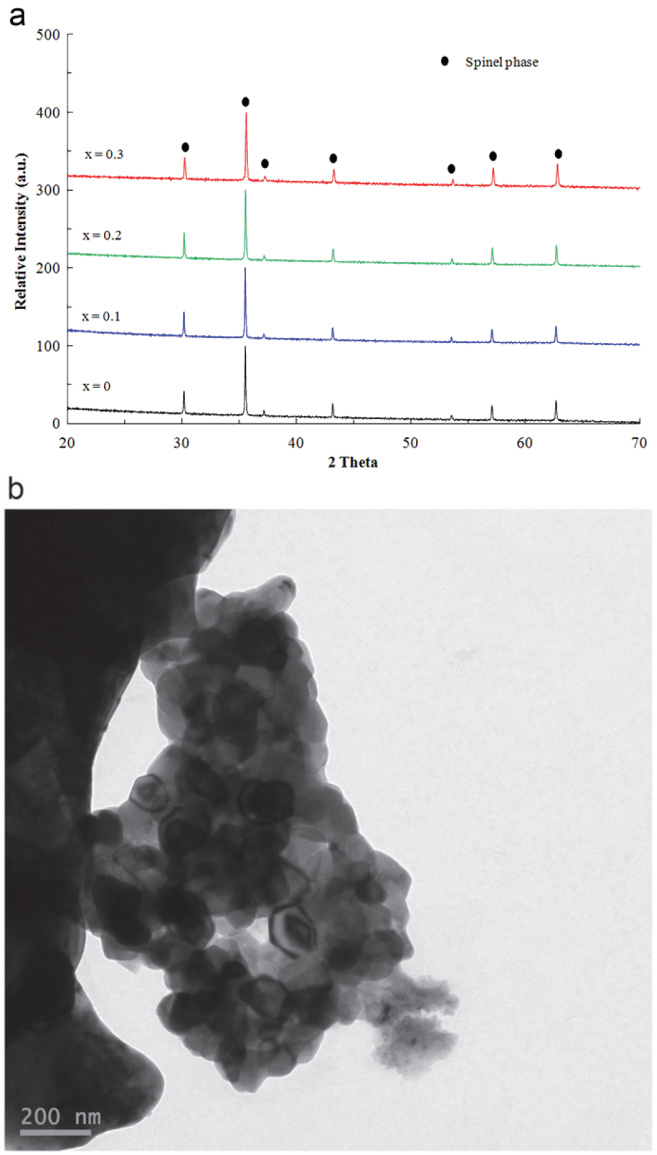

Figure 2. (a) X-ray diffraction spectra of calcined $CoZn_xFe_{2-x}O_4$, (x = 0, 0.1, 0.2, and 0.3); (b) Bright-field TEM image of the calcined $CoFe_2O_4$.

lattice parameter (a) was calculated by Cohen's method [25]. The a value ranges between 8.3000 and 8.5000 Å (Table 1) that is typical of spinel-ferrites. The variation in a in spinel-ferrites depends on the type of metal ions present [11]. The a for $CoFe_2O_4$ (8.3941±0.0008 Å) is similar to a reported for Co-ferrite in the literature [12, 13]. The minor variation in a for $CoFe_2O_4$ among the values reported in the literature and that obtained in the current study is most likely due to the variation in the purity level of the initial raw materials and the method of synthesis of the Co-ferrite. Co-ferrite in its inverse-spinel form would have half Fe^{3+} occupying the tetrahedral site, while the other half Fe^{3+} and the Co^{2+} would occupy the octahedral sites. The site occupation for Fe^{3+} and Co^{2+} ions is known to vary with fabrication processes and hence it is expected to affect a [14, 15]. Substituting Zn for Fe increases the value of a for $CoFe_{2-x}Zn_xO_4$ (x = 0.1, 0.2, and 0.3) as compared to that for $CoFe_2O_4$. Based on the fact that the radius of Zn^{2+} ions in tetrahedral and octahedral sites is greater than that of Fe^{3+} ions, each of the site replacing Fe^{3+} with Zn^{2+} is expected to increase a [16]. However the increase

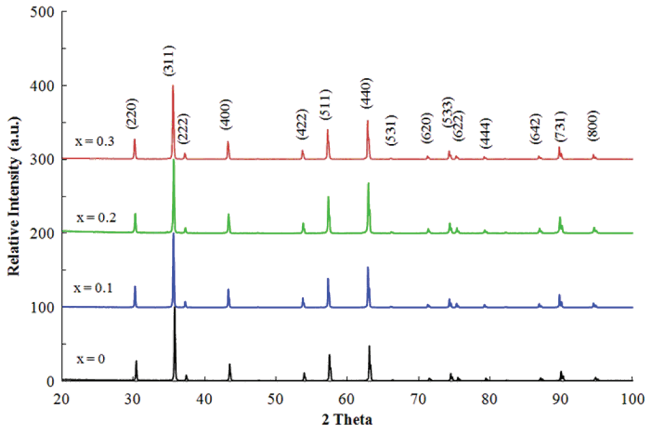

Figure 3. X-ray diffraction spectra of $CoZn_xFe_{2-x}O_4$, (x = 0, 0.1, 0.2, and 0.3) sintered at 1300 °C for 12 h.

Table 1. Lattice parameter (a), saturation magnetization (M_S), coercivity (H_C), saturation magnetostriction (λ_S), and strain sensitivity ($dB/d\sigma$) of $CoFe_{2-x}Zn_xO_4$ (x = 0, 0.1, 0.2, and 0.3).

Material	a (Å) (±0.0008)	M_S (emu/g) (±1%)	H_C (Oe) (±1%)	λ_S (ppm) (±2%)	$dB/d\sigma$ (Oe^{-1})
$CoFe_2O_4$	8.3941	81.6	539	−183	57.5×10^{-9}
$CoFe_{1.9}Zn_{0.1}O_4$	8.4036	84.3	165	−148	105×10^{-9}
$CoFe_{1.8}Zn_{0.2}O_4$	8.3991	86.6	87	−103	85×10^{-9}
$CoFe_{1.7}Zn_{0.3}O_4$	8.4011	81.2	105	−57	50×10^{-9}

in a with increasing Zn composition does not seem to follow the Vegard's law [17, 27]. This suggests that possibly the Zn-doped Co-ferrite in the present study is in a mixed spinel form (neither completely a normal spinel nor an inverse spinel) [18]. Additionally, Zn-ferrites are known to have a normal spinel structure and Co-ferrites are known to have an inverse spinel structure, which suggests a possibility of a mixed spinel structure in Zn-doped Co-ferrite [19]. The non-linear behavior of a for $CoFe_{2-x}Zn_xO_4$ (x = 0.1, 0.2, and 0.3) is similar to previously reported Si, Ga, and Ge substituted Co-ferrites [20]. The correlation between a and the cationic distribution (Zn^{2+}, Co^{2+}, and Fe^{3+}) among tetrahedral and octahedral sites is beyond the scope of the current investigation. However, for a thorough structural characterization the neutron diffraction, EXAFS, and Mossbauer spectroscopy study of the Zn-doped Co-ferrites are currently underway.

Figure 4 shows the SEM micrographs of the Zn doped ferrites, $CoZn_xFe_{2-x}O_4$ (x = 0, 0.1, 0.2, and 0.3), sintered at 1300 °C for 12 h. The average grain size for all the compositions were ~2–4 μm. It is obvious from the micrographs that the grain size of the doped compositions is larger than that of pure cobalt ferrite. The sintering kinetics of the cobalt ferrite seem to be greatly altered in the presence of Zn. Zn, in a divalent cation (Zn^{+2}) form, when doped in the trivalent Fe^{+3} site of the cobalt ferrite lattice creates oxygen vacancies (V_{O}..) in order to maintain the electrical charge neutrality of the crystal. As more and more Zn goes into the Fe sites of the cobalt ferrite lattice, more oxygen vacancies are created. The rate of sintering is enhanced in presence of oxygen vacancies thus facilitating the grain growth.

Figure 5 shows the field dependence of magnetization (M–H) for Zn-doped cobalt-ferrites measured at ambient temperature (~298 K).The saturation magnetization (M_S) and coercivity (H_C) values are listed in Table 1. The M_S for $CoFe_2O_4$ sample is ~82 emu/g; it is close to previously reported saturation magnetization values for Co-ferrites [24]. With increase in Zn substitution, the M_S initially increases from ~82 emu/g (x = 0) to ~87 emu/g (x = 0.2), followed by a subsequent decrease

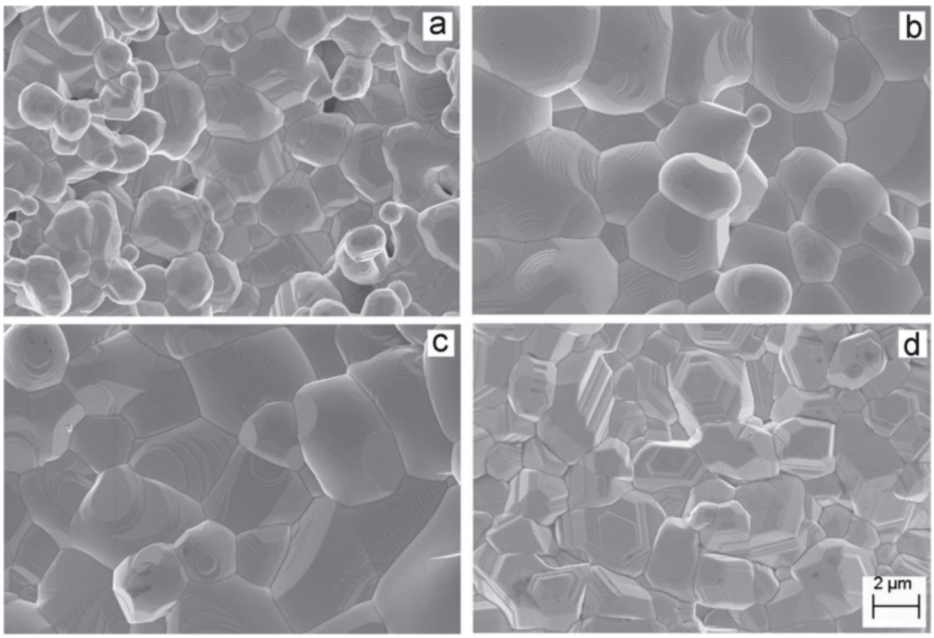

Figure 4. SEM micrographs of (a) $CoFe_2O_4$, (b) $CoFe_{1.9}Zn_{0.1}O_4$, (c) $CoFe_{1.8}Zn_{0.2}O_4$, and (d) $CoFe_{1.7}Zn_{0.3}O_4$, sintered at 1300 °C for 12 h.

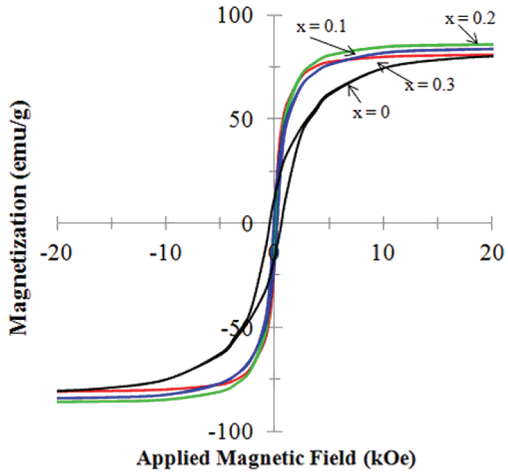

Figure 5. Magnetization (M–H) curves of $CoZn_xFe_{2-x}O_4$, (x = 0, 0.1, 0.2, and 0.3) at ambient temperature (~298 K).

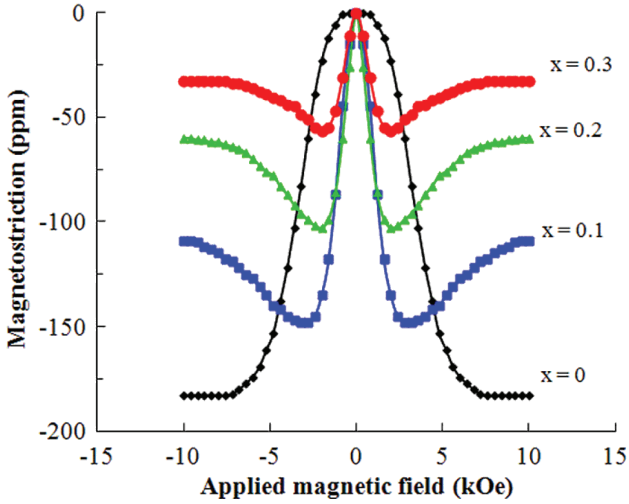

Figure 6. Magnetostriction (λ–H) curves of $CoZn_xFe_{2-x}O_4$, (x = 0, 0.1, 0.2, and 0.3) at ambient temperature (~298 K).

in M_S with increasing Zn content. A similar trend in saturation magnetization is observed in mixed ferrites (MO. Fe_2O_3; M = Mn, Co, Ni) with addition of nonmagnetic Zn^{2+} [24]. The increase in M_S for x = 0 to x = 0.1 is 3.3%, however the increase from x = 0.1 to x = 0.2 is 2.7%. The drop in percentage increase of M_S at x>0.1 suggests the possible contention for Zn^{2+} to go to octahedral sites vs. tetrahedral sites. The coercivity (H_C) of cobalt ferrite in the current investigation is ~525 Oe, which sharply decreases to ~165 Oe for $CoFe_{1.9}Zn_{0.1}O_4$, followed by a gradual decrease in H_C with subsequent Zn addition. The decrease in coercivity is likely associated with the reduction in anisotropy with increasing zinc content in cobalt ferrite [24]. The sudden drop in coercivity from 525 Oe in x = 0 to 165 Oe in x = 0.1 is an indication of a possible change in orientation of the magnetization vector from the easy axis (100) in $CoFe_2O_4$ to the hard axis (111) in $CoFe_{1.9}Zn_{0.1}O_4$.

The magnetostriction curves (Figure 6) for the zinc-doped Co-ferrites samples measured at room temperature reveal that the peak value of magnetostriction decreases with increasing zinc content in cobalt-ferrite. The saturation magnetostriction (λ_S) values are listed in Table 1.The λ_S for $CoFe_2O_4$ is ~−183 ppm. With increasing Zn content the peak value of magnetostriction gradually decreases to ~−57 ppm for $CoFe_{1.7}Zn_{0.3}O_4$. Progressive Zn addition (replacing Fe) to Co-ferrite lattice causes the magnetostriction to decrease substantially beyond its saturaton value, λ_S. The shape of the magnetostriction curves of the Zn-doped cobalt ferrites is different than their undoped counterpart. The large negative slope in the field induced strain (λ) at lower field is due to the dominant contribution from λ_{100} (less than zero for pure cobalt ferrite at room temperature). At higher field λ increases slowly with a positive slope because of the dominant contribution from λ_{111} [24, 28]. Zn doping in the cobalt ferrite causes some magnetization vectors to go away from the easy axis (100) towards the hard axis (111) in order to align the domains at higher applied field. The resulting shift of the magnetization vectors from (100) to (111) is an indication of the decrease in magnetocrystalline anisotropy (anisotropy energy), which corroborates with the observed decrease in coercivity data in the Zn doped cobalt ferrite (Figure 6; Table 1).

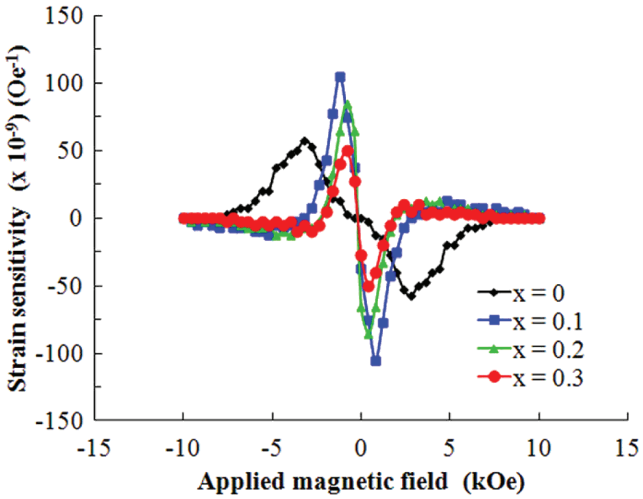

Figure 7. Strain sensitivity ($d\lambda/dH$–H) curves of $CoZn_xFe_{2-x}O_4$, (x = 0, 0.1, 0.2, and 0.3) at ambient temperature (~298 K).

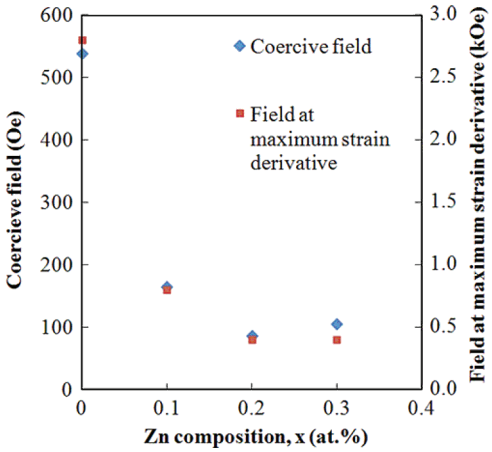

Figure 8. Correlation between coercive field (H_c) and field required to attain maximum strain derivative (H in kOe) for $CoZn_xFe_{2-x}O_4$, (x = 0, 0.1, 0.2, and 0.3).

The variation of strain derivative ($d\lambda/dH$) with applied magnetic field, for Zn-doped cobalt-ferrites, is shown in Figure 7 and the maximum strain sensitivity values are listed in Table 1. The value of strain sensitivity shows a maximum (~105×10^{-9} Oe^{-1}) at an applied magnetic field of ~1.2 kOe for $CoFe_{1.9}Zn_{0.1}O_4$ and then decreases for both x>0.1 and x<0.1. The strain derivative of a magnetostrictive material depends on the ratio of saturation magnetostriction and magnetocrystalline anisotropy and is proportional to their ratio [5]. The relation between the strain derivative and saturation magnetostriction is given by [29]:

$$d\lambda/dH = dB/d\sigma = (2\mu_o\lambda_S M)/(NK) \quad (1)$$

where, μ_o is the initial permeability, λ_S is the saturation magnetostriction, M is the magnetization, K is the anisotropy energy, N is a constant depending on the anisotropy of the material, $d\lambda/dH$ is the piezo magnetic coefficient (strain sensitivity), and $dB/d\sigma$ is the sensitivity of magnetic induction to stress. Therefore, the saturation magnetostriction (λ_S) is not the only factor that decides the performance of these materials as stress (torque) sensor, it is also a function of anisotropy constant (K) of the material. The strain sensitivity of the sample with x = 0.1 is higher than that of pure cobalt ferrite. The reduction in magnetocrystalline anisotropy (K) could be more than the saturation magnetostriction so that λ_S/K is highest for x = 0.1. For the other Zn doped samples (x = 0.2, 0.3) the reduction in magnetocrystalline anisotropy is probably lower (also seen in the coercivity data) than the reduction in saturation magnetostriction. The dependence of the piezomagnetic coefficient (equivalent to stress sensitivity) of the substituted cobalt ferrite on the magnetocrystalline anisotropy (and hence coercive field) is further evidenced by the fact that a similar magnitude of reduction in field requirement (~70% decrease from 2.8 kOe for x = 0 to 0.8 Oe for x = 0.1) to achieve the maximum strain sensitivity has been observed. Similarly ~70% reduction in coercivity is observed for $CoFe_{1.9}Zn_{0.1}O_4$ compared to that for $CoFe_2O_4$. The dependence of coercieve field and the field requirement to attain the maximum strain sensitivity of the Zn substituted cobalt ferrite is shown in Figure 8. An extremely strong correlation between the coercive field and the field required for maximum strain derivative, with increasing Zn content, indicates that the decrease in anistoropy energy (coercivity) with Zn addition plays a major contributor to the observed variation in piezomagnetic coefficient in Zn-doped cobalt ferrite. Besides magnetocrystalline anisotropy other factors including, internal stress and defects such as dislocations and grain-boundary in the crystals of the Zn-doped Co-ferrite affect H_C, $d\lambda/dH$, and $dB/d\sigma$. A comprehensive study of these effects is currently under way.

The present study reveals that Zn-doping in Co-ferrites improves the strain-derative—suggesting their potential application in stress sensors or as stress sensory agent. In this regard the mechanical robustness of the doped materials including resiliance, strength, and toughness play a significant role along with their magnetic and magnetistrictive properties. The mechanical characterization of the doped materials is outside the scope of the current work; however this aspect is currently being dealt for future study. Apparently an important characteristics of magnetoelastic materials from application point of view, other than $d\lambda/dH$ is λ_S. A stable and repetitive value of λ_S is more desirable than $d\lambda/dH$, since the magnetic status at values below saturation magnetization (<λ_S or maximum value of $d\lambda/dH$) may not be adequately stable due to high magnetic field derivative of induction. However, high strain derivative ($d\lambda/dH$) is indicative of the material's potential application as magnetoelastic sensors and/or actuators, particularly where low strain requiring high sensitivity is desired [28, 30]. Furthermore the $d\lambda/dH$ values depends not only on the external H but also on the history of magnetization (initial magnetization, descending and ascending stage). In the present investigation the history of magnetization, particularly the initial stage (permeability), of the Zn doped samples are very different than pure cobalt ferrite as evident in the magnetic hystersis behavior (Figure 5). These facts provide the necessary motivation constructive for future study.

4. Summary and conclusions

Zn-doped cobalt-ferrites, with nominal compositions $CoFe_{2-x}Zn_xO_4$ (x = 0, 0.1, 0.2, and 0.3), were synthesized by auto-combustion technique using Co- , Fe- , and Zn-nitrate as precursors. The as-prepared ferrite powders were comprised of nanostructured cubic-spinel phase (grain size ~45 nm) along with minor impurity phases, as obtained from XRD analysis. TEM study also revealed that the as-prepared powders were nanocrystalline (~25–30 nm) having irregular morphology. Calcination (800 °C for 3 h) of the precursor followed by sintering (1300 °C for 12 h) of the green pellets resulted in a single phase cubic-spinel structure with average grain size

~2–4 μm, as estimated from SEM micrographs. The increase in grain size with increasing Zn doping is a result of enhanced sintering kinetics in presence of oxygen vacancies. Saturation magnetization initially increases from ~81 emu/g for $x = 0$ and peaks to ~87 emu/g for $x = 0.2$ and then decreases. The sharp decrease in coercive field from ~540 Oe for $x = 0$ to ~165 Oe for $x = 0.1$ with a subsequent gradual decrease to ~105 Oe with increasing Zn doping up to $x = 0.3$ is indicative of decreasing anisotropy in the doped cobalt ferrite system. The monotonic decrease in peak value of magnetostriction (from −183 ppm for $x = 0$ to −57 ppm for $x = 0.3$) with increasing Zn content in the range 0.0–0.3 and observed variation in coercivity corroborate the change in orientation of the magnetization vector from the easy axis (100) in undoped Co-Ferrite to the hard axis (111) in Zn-doped Co-ferrite. The observed variation in piezomagnetic coefficient (equivalent to strain derivative), $d\lambda/dH$, with composition (x) in the Zn substituted cobalt ferrite; and its value reaching a maximum at 105×10^{-9} Oe^{-1} for $x = 0.1$, is related to the reduced anisotropy of the system. The Zn-doped cobalt-ferrite ($x = 0.1$) having high strain derivative could be a potential material for stress sensor application.

References

[1] Y. Yin, A. P. Alivisatos, *Nature* 437 (2005) 664.

[2] B. Y. Geng, J. Z. Ma, X. W. Liu, Q. B. Du, M. G. Kong, L. D. Zhang, *Applied Physics Letters* 90 (2007) 043120.

[3] S. Sun, C. B. Murray, D. Weller, L. Folks, A. Moser, *Science* 287 (2000) 1989.

[4] D. C. Jiles, C. C. H. Lo, *Sensors and Actuators A* 106 (2003) .

[5] M. Rajendran, R. C. Pulla, A. K. Bhattacharya, D. Das, S. N. Chintalapudi, C. K. Majumdar, *Journal of Magnetism and Magnetic Materials* 232 (2001) 71.

[6] C. Liu, B. Zou, A. J. Rondinone, Z. J. Zhang, *Journal of the American Chemical Society* 122 (2000) 6263.

[7] Z. J. Zhang, Z. L. Wang, B. C. Chakoumakos, J. S. Yin, *Journal of the American Chemical Society* 120 (1998) 1800.

[8] T. L. Templeton, A. S. Arrott, A. E. Curzon, M. A. Gee, X. Z. Li, Y. Yoshida, P. J. Schurer, J. L. LaCombe, *Journal of Applied Physics* 73 (1993) 6728.

[9] J. CWacrenoborgh, M. O. Figucerido, J. M. P. Cabrol, L. C. J. Pereiro, *Journal of Solid State Chemistry* 111 (1994) 300.

[10] C. Kashinath, Patil, *Current Opinion in Solid State and Materials Science* 6 (2002) 507.

[11] Alex Goldman, *Modern Ferrite Technology,* 2nd ed., Springer Science+Business Media, Inc., 2006, Chapter 4.

[12] M. Sorescu, A. Grabias, D. Tarabasanu-Mihaila, L. Diamandescu, *Journal of Materials Synthesis and Processes* 9 (3) (2001) 119.

[13] W. Bayoumi, *Journal of Materials Science* 42 (2007) 8254.

[14] G. A. Sawatzky, F. Woude, A. H. Morrish, *Journal of Applied Physics* 39 (1968) 1204.

[15] M. McGuire, R. C. O'Handley, G. Kalonji, *Journal of Applied Physics* 65 (1989) 3167.

[16] J. A. Dean, *Lange's Handbook of Chemistry,* 16th ed., McGraw-Hill, New York, 2005.

[17] A. R. Denton, N. W. Ashcroft, *Physical Review A* 43 (1991) 3161.

[18] S. S. Shinde, K. M. Jadhav, *Journal of Materials Science Letters* 17 (1988) 849.

[19] T. F. Barth, W. E. Posnjak, *Zeitschrift für Kristallographie* 82 (1932) 325.

[20] S. H. Song, Doctoral Dissertation, Dept. of Materials Science and Engineering, Iowa State University, Ames, Iowa, 2007.

[21] A. Navrotsky, O. J. Kleppa, *Journal of Inorganic Nuclear Chemistry* 29 (1967) 2701.

[22] L. A. Chick, L. R. Pederson, G. D. Maupin, J. L. Bates, L. E. Thomas, G. J. Exarhos, *Materials Letters* 10 (1990) 6.

[23] S. D. Bhame, P. A. Joy, *Sensors and Actuators A: Physical* 137 (2) (2007) 256.

[24] B. D. Cullity, C. D. Graham, *Introduction to Magnetic Materials*, Wiley/IEEE, NJ, 2009.

[25] R. A. Young, D. B. Wiles, *Journal of Applied Crystallography* 15 (1982) 430.

[26] C. Suryanarayana, M. G. Norton, *'X-RayDiffraction' a Practical Approach,* Plenum Publishing Corporation, New York, 1998.

[27] B. D. Cullity, S. R. Stock, *Elements of X-ray diffraction,* Upper Saddleriver, Wiley, PrenticeHall NJ, 2001.

[28] Naresh Ranvah, I. C. Nlebedim, Y. Melikhov, J. E. Snyder, D. C. Jiles, A. J. Moses, P. I. Williams, F. Anayi, Sang-Hoon Song, *IEEE Transactions on Magnetics* 44 (2008) 3013.

[29] Y. Chen, B. K. Kriegermeier-Sutton, J. E. Snyder, K. W. Dennis, R. W. McCallum, D. C. Jiles, *Journal of Magnetism and Magnetic Materials* 236 (2001) 131.

[30] R. W. McCallum, K. W. Dennis, D. C. Jiles, J. E. Snyder, Y. H. Chen, "Fundamental investigations and industrial applications of magnetostriction," in *Modern Trends in Magnetostriction Study and Application*, M. R. J. Gibbs (ed.), Kluwer Academic Publishers, Netherlands, 2000.